

COSMIC VARIANCE IN THE TRANSPARENCY OF THE INTERGALACTIC MEDIUM AFTER REIONIZATION

J. Stuart B. Wyithe¹ and Abraham Loeb²
swyithe@physics.unimelb.edu.au; aloe@cfa.harvard.edu

Draft version November 2, 2018

ABSTRACT

Following the completion of cosmic reionization, the mean-free-path of ionizing photons was set by a population of Lyman limit absorbers. As the mean-free-path steadily grew, the intensity of the ionizing background also grew, thus lowering the residual neutral fraction of hydrogen in ionization equilibrium throughout the diffuse intergalactic medium (IGM). Lyman photons provide a sensitive probe for tracing the distribution of this residual hydrogen at the end of reionization. Here we calculate the cosmic variance among different lines-of-sight in the distribution of the mean Lyman optical depths. We find fractional variations in the effective post-reionization optical depth that are of order unity on a scale of

100 comoving Mpc, in agreement with observations towards high-redshift quasars. The variations are dominated by the cosmic variance in the density contrast on the scale of the mean-free-path for ionizing photons, and by fluctuations in the ionizing background induced by delayed or enhanced structure formation. Cosmic variance results in a highly asymmetric distribution of transmission through the IGM, with fractional fluctuations in Lyman transmission that are larger than in Lyman transmission.

Subject headings: cosmology: theory – galaxies: formation

1. introduction

It is thought that the appearance of the first galaxies and quasars reionized the cosmic hydrogen in the intergalactic medium (IGM) that was left neutral following the recombination era at $z = 10^3$. The process started with the emergence of ionized regions around galaxies and then groups of galaxies. These H II regions eventually overlapped, leaving the IGM highly ionized in low-density regions surrounding pockets of residual neutral hydrogen in high density regions. The process of reionization was inhomogeneous (Furlanetto et al. 2004), and the overlap should have occurred at different times in different regions (Wyithe & Loeb 2004b). However the identification of a Gunn-Peterson trough in the spectra of the most distant quasars at redshifts of $z = 6.3$ – 6.4 (Fan et al. 2004) hints that the reionization of cosmic hydrogen was completed near $z = 6$, about a billion years after the big bang (Wyithe et al. 2003; Wyithe & Loeb 2004a; Mesinger & Haiman 2004).

Prior to the overlap epoch, the mean-free-path of ionizing photons was limited by the size of individual H II regions. Following overlap, regions of IGM were exposed to ionizing radiation from additional sources. This increase in the ionizing intensity ionized hydrogen in denser regions, and resulted in an increased mean-free-path which in turn led to an even higher ionizing intensity. As the ionizing intensity in the post-overlap IGM rose, the optical depth to Lyman absorption decreased (e.g. Fan et al. 2002). Observations of the absorption spectra of high redshift quasars (Fan et al. 2004) and potentially gamma-ray burst afterglows (Barkana & Loeb 2004; Chen et al. 2005) provide clues to the evolution of the ionizing radiation field and of the evolution of the ionizing photon mean-free-path.

The post-overlap evolution in the IGM is expected to be inhomogeneous. Indeed values of optical depth to

Lyman absorption measured along different lines of sight at $5 < z < 6$ show fluctuations that are of order unity (Becker et al. 2001; Wyithe et al. 2003). The Lyman optical depth therefore varies from place to place at any slice of cosmic time. In addition to small scale variations in Lyman optical depth (the so-called Lyman forest), there would be large scale inhomogeneities in the evolution of the ionization state of the IGM. These large scale variations would be present on the scale of the mean-free-path for ionizing photons (~ 10 – 100 comoving Mpc). Cosmic variance on these scales can be significant and is not described by contemporary numerical simulations of the reionization process (Barkana & Loeb 2004). To model cosmic variance properly with numerical simulations would require resolving low-mass galaxies as well as solving the radiative transfer equations inside a very large box (hundreds of comoving Mpc) with a much higher dynamical range of scales than currently accessible by state-of-the-art codes.

In this paper we examine the variations in the optical depth averaged over a redshift bin of sufficient size to smooth out the small-scale inhomogeneities of the Lyman forest. The variation in optical depth includes several contributions: (i) variations in the density-contrast on the scale of the mean-free-path for ionizing photons, (ii) variations in the ionizing background on the same scale due to enhanced or delayed structure-formation, (iii) variations in the ionizing background due to finite light travel time across the clustering length of ionizing sources, (iv) variations in the ionizing background due to Poisson fluctuations in the number of ionizing sources, and (v) evolution of the density of Lyman limit absorbers. Throughout the paper we adopt the set of cosmological parameters determined by the Wilkinson Microwave Anisotropy Probe (WMAP, Spergel et al. 2003), namely mass density parameters of $\Omega_m = 0.27$ matter, $\Omega_b = 0.044$ in baryons,

¹ University of Melbourne, Parkville, Victoria, Australia² Harvard-Smithsonian Center for Astrophysics, 60 Garden St., Cambridge, MA 02138

$= 0.73$ in a cosmological constant, and a Hubble constant of $H_0 = 71 \text{ km s}^{-1} \text{ Mpc}^{-1}$.

2. fluctuations in ionizing intensity and Ly optical depth

The background intensity of ionizing radiation J (note we assume a universal spectrum because we are averaging over a large number of sources) is proportional to the comoving number density of ionizing sources (n_{src}), the density contrast (δ), the bias of sources in an overdense region (B_{src}) and the comoving mean-free-path for ionizing photons (R_{mfp}),

$$J / n_{\text{src}} (1+z)^3 B_{\text{src}} \frac{R_{\text{mfp}}}{1+z} : \quad (1)$$

The mean-free-path is in turn related to the effective comoving density of Lyman- α absorbers (n_{abs}) as well as their bias (B_{abs})

$$\frac{R_{\text{mfp}}}{1+z} / n_{\text{abs}} (1+z)^3 B_{\text{abs}}^{-1} : \quad (2)$$

We can also relate the average comoving density of sources to the collapsed fraction of baryons F_{col} into dark matter halos above some minimum mass that reflects the threshold for cooling and fragmentation of the gas into stars or accreting black holes), $n_{\text{src}} / F_{\text{col}}$, so that

$$J / \frac{F_{\text{col}} B_{\text{src}}}{n_{\text{abs}} B_{\text{abs}}} : \quad (3)$$

If both sources and absorbers reside in halos of the same mass, then $B_{\text{abs}} = B_{\text{src}}$. This may be the case once the gas in mini-halos below the cooling and fragmentation threshold, has been photo-evaporated. However at high redshifts just after the overlap of H II regions, the mini-halos might provide a significant contribution to the population of Lyman- α absorbers (Barkana & Loeb 2002; Iliev, Shapiro, & Raga 2005). In this case $B_{\text{src}} > B_{\text{abs}}$. These bias factors are expected to evolve with time; B_{src} may have a slow redshift dependence through a changing minimum mass for galaxy formation while B_{abs} may have a value that changes with redshift if the typical absorber mass changes with time (for example if mini-halos are being evaporated) and so B_{abs} could be a function of the evolving J .

Suppose that n_{abs} is some general function of F_{col} and J . If the number density of absorbers was simply proportional to the collapsed fraction, $n_{\text{abs}} / F_{\text{col}}$, then J would be independent of redshift. However Lyman- α systems are expected to shrink in physical cross-section as their lower-density envelopes are ionized by a growing ionizing background. The effective density of absorbers should therefore be a function of J in addition to F_{col} . Equation (3) is therefore an implicit equation for J as a function of F_{col} .

The above considerations lead to two interesting conclusions. First, we find that J should be independent of density contrast at a fixed value of collapsed fraction; and second, the average ionizing background J within a region of radius equal to R_{mfp} should be a function only of the value for F_{col} . With these points in mind we can estimate the scatter in the redshift at which a threshold value of J is reached, and from it find the corresponding scatter in the value of J at fixed redshift.

2.1. Fluctuations due to cosmic variance

Large-scale inhomogeneity in the cosmic density field leads to structure formation that is enhanced in over-dense regions and delayed in under-dense regions. The resulting cosmic variance in the redshift at which a critical value of F_{col} is reached within regions of size R may be calculated as

$$h z_{\text{cv}}^2 i^{\frac{1}{2}} = \frac{R}{c} (1+z); \quad (4)$$

where R is the variance on spheres of radius R , and $c / (1+z)$ at high redshift (Barkana & Loeb 2004; Bond et al. 1991). Since the ionizing background within a given region depends on the value of the collapsed fraction, we can relate $h z_{\text{cv}}^2 i^{\frac{1}{2}}$ to the cosmic variance in redshift where a critical value of J is obtained. The value of J is independent of δ . We therefore use the mean-free-path averaged over all overdensities as the appropriate length scale over which the cosmic variance is calculated, i.e. $R = R_{\text{mfp}} = 2$.

The left panel of Figure 1 shows the scatter in the redshift at which a critical value of J is obtained due to cosmic variance, $h z_{\text{cv}}^2 i$ (solid lines). We would like to convert this scatter in redshift to a scatter in the optical depth to Lyman- α absorption at a given redshift. At a fixed redshift z , the value of Lyman- α optical depth scales as

$$/ \frac{2}{H_0} J^{-1}; \quad (5)$$

where H_0 is the density of neutral hydrogen. While the ionizing background will be sensitive to cosmic variance in density contrast calculated in 3-dimensional volumes (δ) on the scale R_{mfp} , the absorption spectra of quasars probe only lines-of-sight through these volumes. The effective optical depth averaged over a length scale R_{mfp} therefore depends on the density contrast (δ_z) calculated in a thin cylinder at redshift z . Note that although δ varies with z due to the growth factor of density perturbations, we focus here on the scatter in δ_z at a fixed z . The fractional change in the value of the optical depth relative to the average, given a density contrast δ_z , and a delay z in the redshift where the critical collapse fraction is reached is

$$\begin{aligned} \frac{\delta \delta_z}{\delta_z} &= \frac{2}{z} \frac{J(z_{\text{av}})}{J(z_{\text{av}}) - \frac{dJ}{dz} z} - 1 \\ &= \frac{2}{z} 1 - \frac{d \ln J}{dz} z^{-1} - 1 \end{aligned} \quad (6)$$

where δ_z is the average value of optical depth at z_{av} (note that the delay is positive for $z > 1$ and negative for $z < 1$). But $J / F_{\text{col}} n_{\text{abs}}^{-1} (B_{\text{src}} = B_{\text{abs}})$, and taking $n_{\text{abs}} (B_{\text{abs}} = B_{\text{src}}) / (1+z)$ we get

$$= \frac{2}{z} 1 - \frac{d \ln F_{\text{col}}}{dz} \frac{1}{(1+z)} z^{-1} - 1: \quad (7)$$

At this point we specify the value of J . One can observe the average number of Lyman- α systems per unit comoving length along the line-of-sight (R_{LL}). Given the observed distribution of column densities for Lyman- α systems, this distance can be related to the mean free path for Lyman- α photons $R_{\text{mfp}} = R_{\text{LL}} = M_{\text{IR}} \Delta z$ (Miralda-Escude 2003). Storrie-Lombardi et al. (1994) measured the abundance of Lyman- α systems per unit redshift at $z = 4$, $dN_{\text{LL}}/dz = 3:3$, leading to a comoving spacing of $R_{\text{LL}} = [(1+z)c(dt=dz)=3:3]$ for Lyman- α systems along the line-of-sight. The resulting mean-free-path for Lyman- α

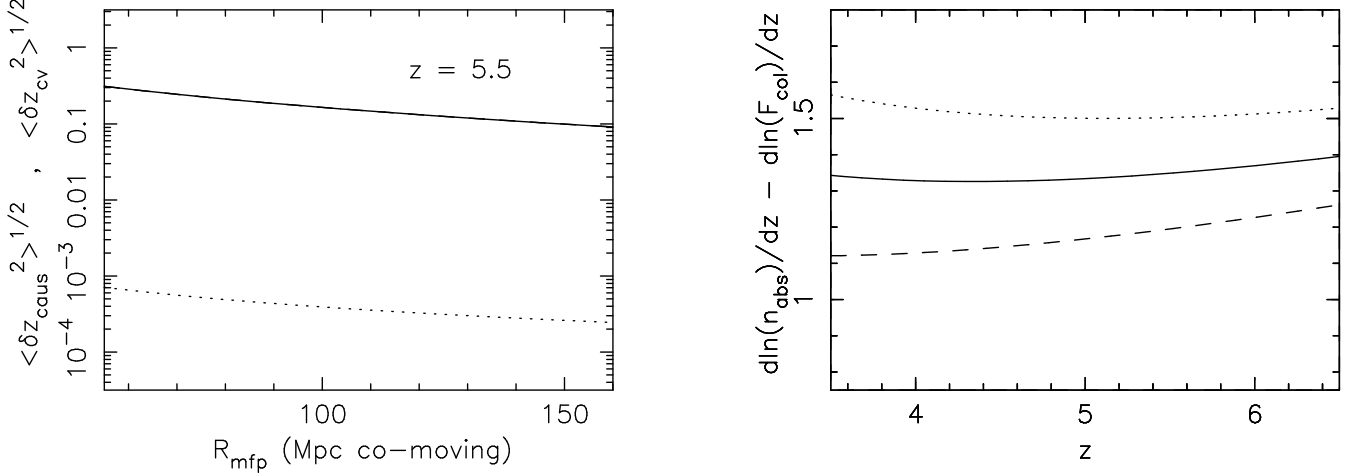


Fig. 1. Left panel: Contribution to scatter in redshift from cosmic variance $h z_{cv}^2 i^{\frac{1}{2}}$ (solid line) and finite light travel time $h z_{caus}^2 i^{\frac{1}{2}}$ (dotted line) as a function of the mean-free-path for ionizing photons in comoving Mpc at a redshift of 5.5. Right panel: The value of $d \ln n_{abs}/dz - d \ln (F_{col})/dz$ as a function of redshift. The dashed, solid and dotted lines correspond to $= 2, 3$, and 4 respectively. In calculating F_{col} we have assumed a minimum virial temperature for galaxies of 2×10^5 K.

photons is $R_{mfp} = 120$ comoving Mpc at $z = 4$. This value provides an upper limit on the mean-free-path for Lyman-alpha photons at higher redshifts when the cosmic gas is denser and less ionized. The evolution of the number of Lyman-alpha systems per redshift is $dN_{LL}/dz = (1+z)^{-1.5}$ (Storrie-Lombardi et al. 1994). The evolution in the number of lines per unit comoving length x is therefore

$$\frac{dN_{LL}}{dx} / (1+z)^{-1} \frac{dN_{LL}}{dz} = \frac{cdt}{dz}^{-1} / (1+z)^{-\frac{3}{2}}; \quad (8)$$

where we have neglected the influence of the cosmological constant at high redshift. The density of absorbers is proportional to dN_{LL}/dx , hence we find $n_{abs} / (1+z)^{-\frac{3}{2}}$, and thus $= + \frac{3}{2}$. The value of β is measured at $z = 4$. However, in halos may be important at high redshift so that an extrapolation of absorption properties from low to high redshift is not justified. We therefore consider a range of values for β which allow for a range of evolutionary properties of the absorbers as well as their bias. In the right panel of Figure 1 we plot the values of the difference between $d \ln F_{col}/dz$ and $d \ln n_{abs}/dz$ as a function of redshift for $\beta = 0.5, 1.5$ and 2.5 ($= 2, 3$ and 4).

In a region of density contrast δ , we can compute the delay due to cosmic variance $\delta z = (1+z)(1-\delta) = c$, leading to a typical delay of $h z_{cv}^2 i^{\frac{1}{2}}$ (see equation 4). However, to estimate the typical fluctuations in the effective optical depth we must also compute the variance in overdensity along lines of sight through the density field of length R_{mfp} . We calculate the power-spectrum of fluctuations in cylinders of length L and radius R to second order in the wave number k (Kaiser & Peacock 1991; Baugh 1996)

$$P_{1d}(k) = \frac{1}{(2\pi)^2} \frac{2}{L} \int_{-k}^{k+L} dy y P_b(y) e^{-(y^2 - k^2)R^2/4}; \quad (9)$$

where $P_b(k)$ is the linear baryonic power-spectrum, which may be approximated as $P_b(k) = P(k)(1+k^2 R_f^2)^{-2}$ in terms of the cold dark matter power-spectrum $P(k)$ and the filtering scale R_f for the associated reionization history (Gnedin & Hui 1998). The variance in δz on a scale R

with wavenumber k_R follows from

$$h z_{cv}^2 i^{\frac{1}{2}} = \frac{1}{2} \int_0^{k_R} dk P_{1d}(k); \quad (10)$$

To estimate typical fluctuations in the optical depth from cosmic variance we assume $\beta = 1$ and δ to be approximately uncorrelated and combine the 1-sigma fluctuation in delay, $h z_{cv}^2 i^{\frac{1}{2}}$, with the 1-sigma fluctuation in density contrast, $\delta z = 1 - R_{mfp} D$ where D is the growth factor, hence

$$h(\delta z_{cv})^2 i^{\frac{1}{2}} = (1 - R_{mfp} D)^2 \quad (11)$$

$$1 - \frac{d \ln F_{col}}{dz} \frac{1}{(1+z)} h z_{cv}^2 i^{\frac{1}{2}} \quad 1:11$$

Figure 2 shows the resulting variation $h(\delta z_{cv})^2 i^{\frac{1}{2}}$, which is monotonic in R_{mfp} .

2.2. Fluctuations due to the finite light travel time

Following the appearance of sources with density n_{src} , the ionizing intensity will grow to its full value J over a timescale $R_{mfp} = [c(1+z)]$ where c is the speed of light. The time when a critical J is achieved is affected by this light propagation delay (with ionizing sources emitting their radiation at a retarded time). However, there may also be a scatter in the time where the critical J is achieved from place to place within the region of comoving size R_{mfp} . This scatter will depend on the distribution of sources. For example, if the sources were clustered on a scale similar to the mean-free-path, then within a region there will be a scatter of $R_{mfp} [(1+z)cdt/dz]^{-1}$ in redshift where the critical J is achieved. However, if the clustering is on a much smaller scale then the scatter will be smaller.

We can estimate this scatter by considering the clustering length of sources, R_0 (which is ~ 4 comoving Mpc for dark matter halos with a virial temperature of $T_{vir} \sim 2 \times 10^5$ K at $z = 5.5$). The photons must travel a distance $R_{mfp} (1+z)^{-1}$ before the critical J is reached. The scatter in arrival times for photons coming from sources clustered on a scale R_0 at a distance R_{mfp} may be estimated as the crossing time of the smaller clustering length

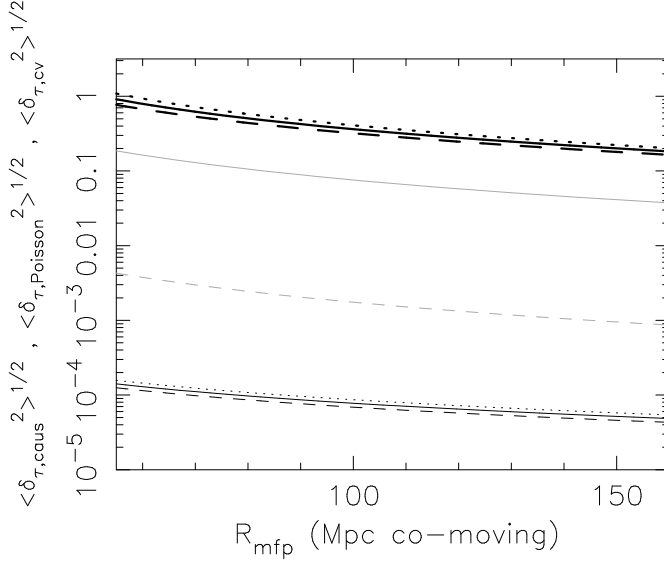


Fig. 2. Contributions to fluctuations in optical depth. The thick lines show the fluctuations in optical depth induced through cosmological variance, $h^2_{;cv} i^{1/2}$. The dashed, solid and dotted lines correspond to $i = 2, 3$, and 4 respectively, and for calculation of F_{col} we have assumed a minimum virial temperature for galaxies of $2 \times 10^5 \text{ K}$. The values of $h^2_{;Poisson} i^{1/2}$ are shown by the light lines; the solid and dashed lines correspond to $t_{Ll} = t_H = 0.01$ and $t_{Ll} = t_H = 0.1$, combined with minimum virial temperatures for galaxies of $2 \times 10^5 \text{ K}$ and 10^4 K respectively. We also show the values of $h^2_{;caus} i^{1/2}$ (dark lines with dashed, solid and dotted curves corresponding to $i = 2, 3$, and 4 respectively). $h^2_{;caus} i^{1/2}$ is much smaller than $h^2_{;Poisson} i^{1/2}$ and $h^2_{;cv} i^{1/2}$. In each case we have evaluated the values of F_{col} at $z = 5.5$.

$(R_0 = c)$ divided by the square-root of the number (N_{cluster}) of clustered regions at a distance R_{mfp} (where the last factor corresponds to Poisson fluctuations in the distances of the clustered regions). Hence the variance in redshift where the critical J is reached due to the light propagation delay will therefore be

$$h z_{\text{caus}}^2 i^{\frac{1}{2}} = p \frac{R_0}{N_{\text{cluster}} (1+z)} \frac{dt}{dz} ; \quad (12)$$

where N_{cluster} is estimated as

$$N_{\text{cluster}} = \frac{4 (R_{\text{mfp}} = 2)^2 R_0}{4 = 3 R_0^3} = \frac{3}{4} \frac{R_{\text{mfp}}}{R_0}^2 ; \quad (13)$$

The corresponding redshift variance due to the light propagation delay $h z_{\text{caus}}^2 i^{\frac{1}{2}}$ is shown on the left panel of Figure 1. At a fixed density contrast, the finite light travel time will introduce a scatter in the value of J of

$$h^2_{;caus} i^{\frac{1}{2}} = 1 + \frac{d \ln F_{col}}{dz} \frac{1}{(1+z)} h z_{\text{caus}}^2 i^{\frac{1}{2}} ; \quad (14)$$

We find that the fluctuations in optical depth due to this effect are much smaller than those due to cosmological variance (see Figure 2).

2.3. Fluctuations due to the finite number of ionizing sources

In addition to the fluctuations in the density and ionizing radiation introduced by cosmological variance and the light propagation delay, we expect a spatial variation of the ionizing intensity due to Poisson noise in the number of ionizing sources within a region of size R_{mfp} . We estimate the number of galaxies using the Press-Schechter (1974) mass function $dN_{PS} = dM$ (with the modification of Sheth & Tormen 1999) and evaluate the number per logarithm of mass

at the minimum mass for galaxy formation (M_{min}). The number of ionizing sources at a particular epoch is given by

$$N_{\text{src}} = \frac{t_{Ll}}{t_H} \frac{dN_{PS}}{d \ln M} \frac{4}{3} \frac{R_{\text{mfp}}}{M_{\text{min}}}^3 ; \quad (15)$$

where t_{Ll} is the source lifetime and t_H is the Hubble time at redshift z . In estimating the fluctuations due to variations in the source numbers we consider two limiting cases. First, we adopt $t_{Ll} = t_H = 0.01$ corresponding to starburst lifetimes of 10^7 years at $z = 5.5$ (the lifetimes of massive stars) and a minimum mass corresponding to the Jeans mass in a photo-ionized IGM (halo virial temperature of $2 \times 10^5 \text{ K}$).

This case corresponds to the smallest source numbers and hence the largest level of Poisson fluctuations in J . Second we consider $t_{Ll} = t_H = 0.1$ corresponding to starburst lifetimes of 10^8 years (of order the orbital time for a circular orbit in a star-forming disk that occupies 10% of the virial radius of its host halo). This lifetime is combined with a minimum halo mass having a virial temperature of 10^4 K , corresponding to cooling threshold of atomic hydrogen (so that the filtering scale is assumed not to have had time to respond to the re-heated IGM). This case corresponds to the largest source numbers and hence to the smallest fluctuations in J . The Poisson noise in the number of galaxies is $N_{\text{src}} = \frac{1}{N_{\text{src}}}$, so that the fluctuations in the optical depth induced by Poisson fluctuations in the number of sources is

$$h^2_{;Poisson} i^{\frac{1}{2}} = \frac{\frac{\partial \ln}{\partial N_{\text{src}}} N_{\text{src}}^2}{N_{\text{src}}} = \frac{\frac{\partial \ln J}{\partial N_{\text{src}}} N_{\text{src}}^2}{N_{\text{src}}} = \frac{\frac{\partial \ln N_{\text{src}}}{\partial N_{\text{src}}} N_{\text{src}}^2}{N_{\text{src}}} = \frac{1}{N_{\text{src}}} ; \quad (16)$$

where we have used the relation J / N_{src} , and evaluated the fluctuation range of corresponding to the 1-sigma a

level of fluctuations in the number counts of sources. The resulting curves are plotted as a function of R_{mfp} in Figure 2.

2.4. Fluctuations in the optical depth

The contributions to the redshift variance introduced by causality, by cosmic variance and by source count fluctuations are independent of each other. The range of allowed σ may therefore be estimated by adding these contributions in quadrature,

$$\sigma = \sqrt{h(\sigma_{\text{cv}})^2 + h^2 \sigma_{\text{caus}}^2 + h^2 \sigma_{\text{Poisson}}^2} \quad (17)$$

3. results and discussion

The upper and lower limits that bracket the range of σ at $z = 5.5$ are plotted in Figure 3. The dashed, solid and dotted lines correspond to $\sigma = 2, 3$ and 4 respectively. The left and right panels show the cases of $t_{\text{Ly}} = t_{\text{H}} = 0.01$ and 0.1 , combined with minimum galaxy masses corresponding to virial temperatures of $2 \times 10^5 \text{ K}$ and 10^4 K respectively. Figure 3 shows that cosmic variance introduces fluctuations in σ that are of order unity over a range of length scales. As the mean free path increases the fluctuations become smaller in line with the smaller cosmic variance on large scales. The fluctuations in σ introduced by fluctuations in the number of sources provides a small contribution. This is in contrast to the situation for double reionization of helium at lower redshifts where the ionizing sources (quasars) reside in rarer more massive systems (Bolton et al. 2005).

The finding that cosmic variance should result in significant fluctuations in σ is qualitatively insensitive to variations in the value of σ (which parameterizes unknowns regarding the absorber properties) over a wide range. This insensitivity arises partly because the collapsed fraction evolves much more rapidly than a power-law with redshift (because the minimum galaxy mass lies on the exponential tail of the Gaussian density distribution), and partly because the fluctuations are dominated by the σ_z^2 term in the evaluation of σ .

We may take the upper limit for R_{mfp} after reionization to be 120 comoving Mpc, which is the value measured at $z = 4$ (Miralda-Escude et al. 2003), while the lower limit is set by the size of bubbles at the end of the overlap epoch (~ 70 comoving Mpc at $z = 6$ and larger if reionization completed earlier; White & Loeb 2004b). The shaded region in Figure 3 delineates the range for different values of R_{mfp} assuming $\sigma = 3$. We find our main conclusion, that cosmic variance introduces large fluctuations in the transmission of the IGM at $z = 5.5$, holds over this full allowed range of Lyman limit mean-free-paths. The reionization redshift itself is also inhomogeneous, as evidenced by the transmission of Lyman-alpha in the Lyman-alpha troughs of some but not all of the $z > 6$ quasars (White et al. 2003; Oh & Furlanetto 2004). Our model becomes applicable at the redshift where most lines of sight probe the post-overlap IGM. Finally, we note that our results do not depend on the reionization redshift having occurred near $z = 6$ but apply to earlier reionization epochs as well.

3.1. Scatter in the transmitted intensity

The scatter in the relative intensity (I / e^{σ}) transmitted through the IGM ($I = (I - I_{\text{av}})/I_{\text{av}}$) is related to the variance in σ through

$$I = \frac{I - I_{\text{av}}}{I_{\text{av}}} = \frac{e^{(\sigma_{\text{av}} + \sigma_{\text{av}})}}{e^{\sigma_{\text{av}}}} - 1; \quad (18)$$

where σ_{av} is evaluated in equation (17). Note that in regions where the optical depth is reduced ($\sigma < 0$) the exponential is positive and the value of I can become very large. For values of optical depth larger than unity the exponential acts as a non-linear amplifier of any inhomogeneities in the IGM which skews the distribution of transmitted intensity. Cosmic variance therefore leads to a highly asymmetric distribution of transmitted flux, even if the distribution of σ is a symmetric Gaussian. For large values of σ ($\gtrsim 5$ immediately following reionization, the variations in the transmission span an order of magnitude. At later times when the optical depth becomes small, equation (18) becomes

$$I \approx 1 - \frac{\sigma_{\text{av}}^2}{2}; \quad (19)$$

Thus at small values of optical depth the distribution of transmitted intensity becomes symmetric.

3.2. Comparison with observations

The results presented in Figure 3 may be compared with existing observations of high redshift quasars. Becker et al. (2001) and White et al. (2003) calculated the effective Lyman-alpha optical depth in bins of width $\Delta z = 0.2$ along the lines of sight to five high redshift quasars. The resulting values of σ for these five lines of sight in the redshift bin $5.5 \leq z \leq 5.7$ are plotted over the grey region in Figure 3 for comparison. At $z = 5.6$ White et al. (2003) find $\sigma_{\text{av}} = 2.5$ and fractional fluctuations in optical depth with values up to $(\sigma_{\text{av}} - \sigma_{\text{av}})/\sigma_{\text{av}} = 0.25$. Since there are only 5 lines of sight we would expect this observed range to be roughly equivalent to the 1-sigma fluctuations plotted in Figure 3, for which we find $\sigma_{\text{av}} = 0.2 - 0.5$. Inspection of Figure 3 therefore suggests that the model is in good agreement with current data. At $z = 5.5$, the redshift bin width of $\Delta z = 0.2$ corresponds to a comoving line-of-sight distance $R_{\text{mfp}} = (1+z)cdt/dz = z = 100$ Mpc. Thus the observations sample the IGM over a length-scale comparable to R_{mfp} , and so are fortuitously matched to our calculation. Of course at redshifts where $R_{\text{mfp}} < 100$ Mpc, our estimate of σ may be compared with observation by averaging the predicted fluctuations over a number [100 Mpc] of regions.

3.3. Relative absorption of Lyman-alpha and Lyman-beta photons

The relative level of absorption for Lyman-alpha and Lyman-beta photons is dictated by the ratio of the product of oscillator strengths and resonance wavelengths for the two transitions. Assuming a homogeneous IGM this results in a Lyman-alpha optical depth that is 6.25 times the Lyman-beta optical depth (Songaila 2004). However the ratio is decreased in an inhomogeneous IGM because on small scales transmission is dominated by low-density regions, while the transition with the lower cross-section for absorption is able to sample a larger range of densities. Oh & Furlanetto (2004) find that values of 2-2.5 are more realistic for the ratio of Lyman-alpha to Lyman-beta optical depth.

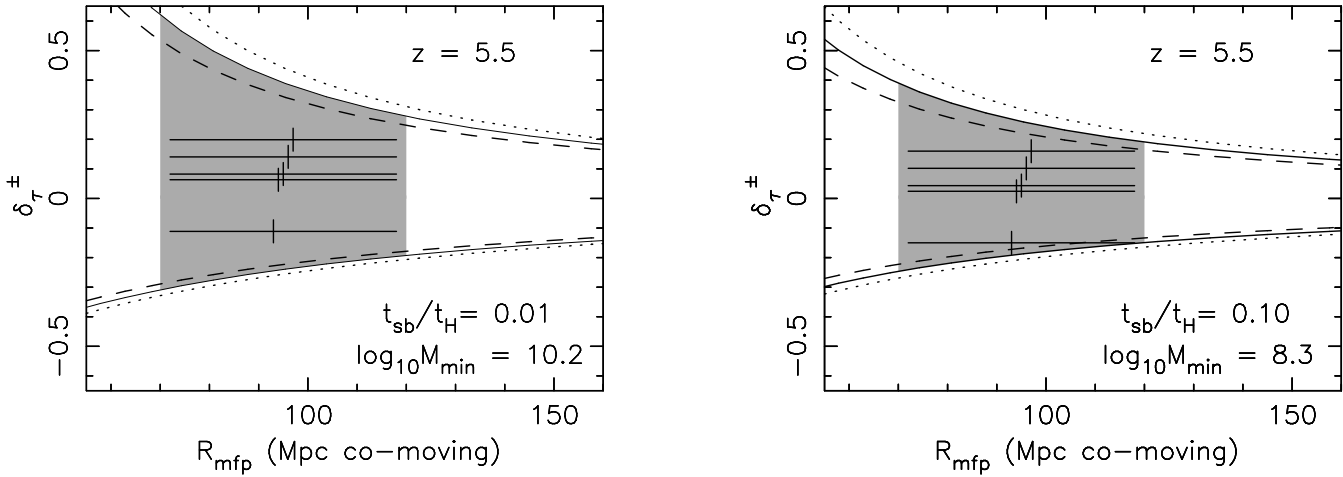


Fig. 3.1 The upper and lower values of the 1-sigma range for fluctuations in τ . The dashed, solid and dotted lines correspond to $\tau = 2, 3$ and 4 respectively. The grey region is bounded from the left by the boundary at 70 co-moving Mpc corresponding to the bubble size at the end of the reionization, and from the right by the ionizing photon mean-free-path at $z = 4$. We show cases with $z = 5.5$, and take populations of ionizing sources having $t_{\text{Ly}} = t_{\text{H}} = 0.01$ (left) and 0.1 (right), combined with minimum galaxy masses corresponding to virial temperatures of 2×10^5 K and 10^4 K respectively. The values of τ at $z = 5.6$ measured along the lines-of-sight to five high-redshift quasars (White et al. 2003) are overplotted. The horizontal error-bars on these observations indicate the possible range of R_{mfp} .

The constant of proportionality relating τ and J will therefore be dependent on the oscillator strength and resonance frequencies. This constant cancels in calculation of τ , and so the range of fractional variation in optical depth will be the same for absorption in Ly α and Ly β . On the other hand the range of optical depth values is given by τ_{av} . As a result, the absolute range of optical depths observed for Ly α absorption will be larger than the range observed for Ly β absorption by a factor of $\sim 2 - 6$. Similarly, while the relative fluctuations in the optical depth are the same for all transitions, we find that the relative fluctuations in observed intensity I will be much larger for Ly β than Ly α photons due to the non-linearity of the exponential relation between optical depth and transmission. In particular, if the Ly β optical depth is smaller than unity, then $I_{\text{Ly}\beta} / \tau_{\text{av}}$ and the relative fluctuations in intensity may be calculated directly from the ratios of the optical depths among the different transitions. In cases where the Ly β optical depth is larger than unity, the variation in I among the different transitions is larger due to the presence of the exponential in equation (18).

4. summary

In this paper we have calculated the magnitude of the large scale fluctuations in the optical depth to absorption of Ly-series photons that are introduced through variance in the cosmological density field. We find that cosmological variance introduces fractional fluctuations in the optical depth that are of order unity for mean-free paths of ionizing photons $R_{\text{mfp}} < 150$ co-moving Mpc. This finding explains the variation seen in the Ly α optical depth along different

lines of sight through the IGM at $z < 6$ (Becker et al. 2001; White et al. 2003).

Our model was not constructed to predict the value of optical depth or to associate a value of the optical depth with the mean-free-path. Rather, it predicts the trend that the relative fluctuations in optical depth will drop as the ionizing photon mean-free-path grows. The mean-free-path increases with cosmic time, and so the range of optical depth will therefore decrease towards low redshift. In addition, while our model predicts a distribution of optical depths that is roughly symmetric about the average, the exponential dependence of transmission on optical depth implies a distribution of transmission that will be highly asymmetric. This asymmetry will become smaller as the average value of optical depth declines at late times. Finally, our model predicts that the absolute fluctuations in the Ly α optical depth should be greater than in the Ly β optical depth. This translates to relative fluctuations in the transmission through the IGM that are much larger for Ly α than for Ly β .

As larger numbers of high redshift quasars are discovered through surveys like the Sloan Digital Sky Survey, the statistics of absorption averaged over large scales will be measured along many lines of sight. The results of this paper suggest that the effects of cosmic variance on the post-reionization epoch will be directly observed in these studies.

The authors would like to thank Xiaohui Fan for pointing out an error in an early version of this manuscript. JSBW acknowledges the support of the Australian research council. This work was supported in part by NASA grants NAG 5-13292 and NNG 05GH54G for AL.

REFERENCES

Barkana, R., Loeb, A., 2002, *ApJ*, 578, 1
 Baugh, C. M., 2004, *ApJ*, 601, 64

Baugh, C. M., 1996, *MNRAS*, 282, 1413

Becker, R. H., et al. 2001, *AJ*, 122, 2850

Bolton, J. S., Haehnelt, M. G., Viel, M., & Carswell, R. F. 2005, *MNRAS*, submitted; astro-ph/0508201

Bond, J.R., Cole, S., Efstathiou, G. & Kaiser, N., 1991, *ApJ*, 379, 440

Chen, H.-W., Prochaska, J. X., Bloom, J. S., & Thompson, I. B., 2005, *ApJL*, submitted; astro-ph/0508270

Fan, X., Narayanan, V. K., Strauss, M. A., White, R. L., Becker, R. H., Pentericci, L., & Rix, H.-W., 2002, *AJ*, 123, 1247

Fan, X., et al. 2004, *AJ*, 128, 515

Furlanetto, S. R., Hernquist, L., & Zaldarriaga, M., 2004, *MNRAS*, 354, 695

Gnedin, N. Y., & Hui, L., 1998, *MNRAS*, 296, 44

Iliev, I. T., Shapiro, P. R., & Raga, A. C., 2005, *MNRAS*, 361, 405

Kaiser, N., & Peacock, J. A., 1991, *ApJ*, 379, 482

Mesinger, A., & Haiman, Z., 2004, *ApJL*, in press, astro-ph/0406188

Miralda-Escude, J., 2003, *ApJ*, 597, 66

Oh, S. P., & Furlanetto, S. R., 2005, *ApJ*, 620, L9

Press, W., Schechter, P., 1974, *ApJ*, 187, 425

Sheth, R. K. & Tormen, G., 1999, *MNRAS*, 308, 119

Songaila, A., 2004, *AJ*, 127, 2598

Spergel, D. N., et al., 2003, *Astron. J. Supp.*, 148, 175

Storrie-Lombardi, L. J., McMahon, R. G., Irwin, M. J., & Hazard, C., 1994, *ApJ*, 427, L13

White, R., Becker, R., Fan, X., Strauss, M., 2003, *Astron. J.*, 126, 1

Wyithe, J.S.B., Loeb, A., 2004a, *Nature*, 427, 815

Wyithe, J. S. B., Loeb, A., 2004b, *Nature*, 427, 815